Spectral and Density Functional Studies on the Absorbance and Fluorescence Spectra of 2-*R*-5-Phenyl-1,3,4-oxadiazoles and Their Conjugate Acids

Alexander V. Gaenko,[†,‡] Ajitha Devarajan,[*,†] Rostislav E. Trifonov,[‡] and Vladimir A. Ostrovskii

Department of Theoretical Chemistry, Chemical Center, Lund University, P.O. Box 124, S-221 00 Lund, Sweden, and St. Petersburg State Institute of Technology (Technical University), 190013, Moskovskii av. 26, St. Petersburg, Russia

Received: February 23, 2006; In Final Form: May 12, 2006

Absorption and fluorescence spectra of 2-R-5-phenyl-1,3,4-oxadiazoles (R = H, methyl, *tert*-butyl, trifluoromethyl, amino, phenyl, benzyl) were studied experimentally and by time dependent density functional theory (TDDFT) methods. In acidic media a substantial red shift is observed due to the presence of conjugate acid forms. Two conjugate acid forms (3H and 4H) are possible for unsymmetrically substituted oxadiazoles. Relative basicities of the two basic centers of oxadiazole ring at the S_0 and S_1 geometries were calculated using the local density descriptors approach. Substituent effects were studied by analyzing the electron density distribution in the ground and excited states. Analyzing the absorption spectra and local descriptors results, we predict 4H forms to be the dominant acid forms. Calculated emission peaks of 4H forms agree well with experimental observations. An abnormal red shift in the case of the 3H forms is attributed to the increased stabilization of the N−H bond in the 3H forms compared to the 4H forms.

1. Introduction

The oxadiazole nucleus is a ubiquitous feature of many pharmacological activities as anti-TB, anti-inflammatory, antibacterial, anti-cancer and anti-HIV.[1,2] 1,3,4-Oxadiazole derivatives have been widely studied in diverse areas of chemistry, in particular due to the electron-deficient properties of oxadiazole ring and their luminescent properties.[3−6] Derivatives of 5-phenyl-1,3,4-oxadiazole are efficient electron transport materials. The spectral properties are essentially acidity dependent, which is due to the acid−base equilibria of the heterocyclic group both in the ground state and in the first excited singlet state. There are very few studies on the effect of medium acidity on the luminescent properties of 5-phenyl-1,3,4-oxadiazoles.[7]

The basicity centers of the oxadiazole derivatives are the pyridine-like nitrogen atoms of the heterocycles.[8] Protonation on the oxygen atom is unlikely, because the resulting cationic form is very unstable. Thus, there are two sites of protonation possible for the unsymmetrically substituted oxadiazoles at N(3) and N(4) nitrogen atoms of the oxadiazole ring. In the case of oxadiazoles having two equal basic centers, such as 2,5-diphenyl-1,3,4-oxadiazoles, protonation leads to only one form of conjugate acid. While studying the luminescent properties of these derivatives in acidic media, one has to consider the protonation of both ground and excited states.

Theoretical studies on luminescence properties and energies of ionization of the oxazoles and oxadiazole derivatives were calculated at best at the semiempirical level.[7,9,10] Kenny[11] have predicted the acceptor power (K_β) of oxazole ring with respect to proton in hydrogen bonding based on molecular electrostatic properties. Only recently reliable ab initio methods based on density functional theory are available to optimize the excited states and evaluate the excited state properties for reasonably big organic molecules.[12−16]

Recently, Parr et al.[17] have proposed a new quantitative definition of global electrophilicity to predict the intermolecular reactivity trends. Domingo[18] has extended the concept of global electrophilicity index to define the local electrophilicity index and successfully explained the regioselectivity in Diels−Alder reactions. To find out the most preferable site (or atom) to be attacked by a nucleophile (or electrophile), Roy[19] proposed the relative electrophilicity (nucleophilicity) descriptors. In the present work we have used the local descriptors to predict the preferred site of protonation in the ground and excited states.

In the present work we have investigated the absorbance and fluorescence properties of 2-R-5-phenyl-1,3,4-oxadiazoles in different water−sulfuric acid mixtures, ethanol and heptane. The absorbance spectra for the neutral and protonated species of the seven derivatives of 2-R-5-phenyl-1,3,4-oxadiazoles were calculated at the ground state optimized geometry and the emission frequency was calculated at the singlet excited state optimized geometry using density functional methods. The solvent effects on the spectra of the basic forms were calculated using the polarizable continuum model. The predominant conjugate acid form was determined by comparing the experimental spectra with the calculated spectra of the 3H and 4H forms. Dominant conjugate acid forms in the ground and excited states were also predicted on the basis of local descriptors. The effect of substituent on the spectra is analyzed on the basis of the excited state density redistributions. Leading transitions contributing to the intense peak in the spectra are also analyzed.

The present article is organized as follows: In section 2, a brief background of the recently developed density based local descriptors for predicting the preferred site of protonation in the ground and excited states is described. In section 3, a brief description of experimental details, structural formulas and the procedure used in calculating spectral properties is presented.

* Corresponding author. E-mail:adevarajan@mail.chem.und.nodak.edu.
† Lund University.
‡ St. Petersburg State University of Technology.

10.1021/jp061174r CCC: $33.50
Published on Web 06/23/2006

In section 4, the results are presented and the theoretical predictions based on calculated spectra and local descriptors are compared with the experimental findings. Finally, in section 5, the remarks on the sites of protonation based on the spectral and descriptors study effect of solvent on the spectral properties of basic and conjugate acid forms are summarized, and conclusions are drawn on the basis of the obtained results.

2. Site of Protonation by Local Softness Values

Although intermolecular reactivity trends can be described by global electrophilicity index (w), the local reactivity or site selectivity of a chemical species are described by local reactivity descriptors, and Fukui function indices[20] $f(\bar{r})$ is one such descriptor.

The global electrophilicity descriptor w is defined as

$$w = \frac{\mu^2}{2\eta} \tag{1}$$

where μ is the chemical potential and η is the global chemical hardness of the chemical system. In the finite difference approximation, we have $\mu \approx -(\mathrm{IP} + \mathrm{EA})/2$ and $\eta \approx (\mathrm{IP} - \mathrm{EA})/2$. Global softness S is defined as $S = 1/2\eta$.

The local reactivity descriptor, Fukui function index $f(\bar{r})$, is defined as

$$f(\bar{r}) = \left(\frac{\partial \rho(\bar{r})}{\partial N}\right)_{v(\bar{r})} = \left(\frac{\partial \mu}{\partial v(\bar{r})}\right)_N \tag{2}$$

where N and $\rho(\bar{r})$ represent the number of electrons and the electron density at position $\bar{r}$ of the chemical species.

The "condensed to atoms" approximation of Fukui function indices, and the global softness values together define the local softness values (s_k) for a nucleophilic, electrophilic and radical attack on the system according to the following equations.

$$s_k^+ = f_k^+ S = [p_k(N+1) - p_k(N)]S \quad \text{(for nucleophilic attack)} \tag{3}$$

$$s_k^- = f_k^- S = [p_k(N) - p_k(N-1)]S \quad \text{(for electrophilic attack)} \tag{4}$$

$$s_k^0 = f_k^0 S = 1/2[p_k(N+1) - p_k(N-1)]S \quad \text{(for radical attack)} \tag{5}$$

where $p_k(N)$, $p_k(N-1)$, and $p_k(N+1)$ represent the condensed electronic populations of atom k for neutral, cationic, and anionic systems, respectively. s_k^+, s_k^-, and s_k^0 represent condensed local softness values, indicating that the atom k is more susceptible toward attack by nucleophile, electrophile and radical on it, respectively. One of the authors[21] has used the local softness values to predict the most favorable adsorption sites for the small molecules on zeolites.

It is worth noting, however, that for predicting the site selectivity, when the reaction centers belongs to the same molecule, both the Fukui function indices and the local softness values obviously provide equivalent information.[22] Recent studies by Roy[23] showed that local softness descriptors, although being not reliable in estimating relative reactivity of molecules (intermolecular reactivity), may be more trustworthy in assessing site selectivity (intramolecular reactivity). We have used the condensed to atoms local softness values to predict the preferred site of protonation when forming a conjugate acid (protonated form).

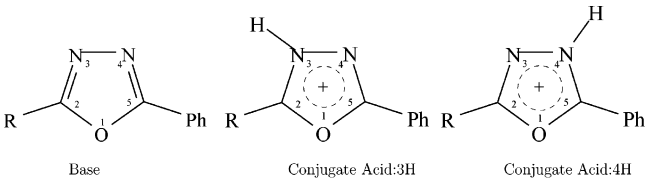

Figure 1. Basic and conjugate acid forms of the studied oxadizaoles.

3. Experimental and Computational Details

3.1. Experimental Details. For our study we have chosen seven substituted monophenyl-1,3,4-oxadiazoles with substituents being H, CH_3, $C(CH_3)_3$, CF_3, NH_2, Ph, $PhCH_2$ groups. Absorption and emission spectra were recorded on Shimadzu UV-2401 and HITACHI F4010 spectrometers, respectively. An aqueous solution of L-tryptophane was used as a standard ($\phi_0 = 0.13$). The excitation of compounds was performed at wavelengths 248 nm, and at the same optical density of the solutions.

3.2. Computational Details. The general structural formulas for the basic form and the two possible conjugate acid forms of the above-mentioned compounds are shown in Figure 1 along with the numeration of atoms used in the present paper.

The ground state geometries of basic and conjugate acid (protonated) forms (3H and 4H) of derivatives of phenyl-1,3,4-oxadiazole were optimized with no symmetry at the RI-DFT level[13] using BP-86 functional.[24−28] We have used the TZVP basis[29,30] for all atoms. The ground state energy and the absorption spectra were calculated using the TDDFT method[16] with B3-LYP functional.[24,26−28,31,32] We have calculated 15 low-lying singlet states. The lowest excitation energy at the optimized geometry corresponds to the absorption frequency of the basic ($\nu_{\mathrm{abs}}^{\mathrm{B}}$) and protonated forms ($\nu_{\mathrm{abs}}^{\mathrm{BH+}}$ (3H, 4H)), respectively.

To calculate fluorescence properties, the geometry of the first excited singlet state S_1 of the basic and the protonated forms were obtained using the TDDFT method for the excited state properties[14] with B3LYP functional. The energy difference between the ground and first excited state at the excited state geometry of basic and conjugate forms corresponds to the observed emission frequency of the basic ($\nu_{\mathrm{fl}}^{\mathrm{B}}$) and conjugate acid forms ($\nu_{\mathrm{fl}}^{\mathrm{BH+}}$ (3H, 4H)), respectively.

Among the substituents chosen for the present study, NH_2, $PhCH_2$, CH_3, $C(CH_3)_3$ are donors of increasing magnitudes, H is neutral and CF_3 is an electron acceptor. Phenyl is a weak σ-acceptor and π-donor substituent.

To estimate qualitatively the relative proton affinity of the base forms, we have calculated the local reactivity descriptors for the ground and excited states of the basic forms based on the Mulliken population analysis (MPA). The low lying orbitals involved in the leading transitions in the absorption spectra of basic and conjugate acid forms were analyzed.

Effect of solvent on the energetics of the basic and conjugate acid forms for CF_3, H and NH_2 derivatives using COSMO polarizable continuum model[33] with $\epsilon = 80$ (corresponds to water as well as dilute sulfuric acid) was estimated. To estimate the effect of solvent on spectra, the response calculation was performed with the solvation model applied to the ground state (we followed the approach taken by Kundrat[34]). It should, however, be noted that this approach takes into account the leading effect of the solvent on the DFT orbitals, but not the

TABLE 1: Gas-Phase Energy Values of Bases (E_B) and Conjugate Acids (E_{3H},E_{4H})

R	base (au)	$E_B - E_{(3H)}$ (kcal/mol)	$E_B - E_{(4H)}$ (kcal/mol)	$E_{(4H)} - E_{(3H)}$ (kcal/mol)
H	−493.0379	−219.9	−223.9	−3.9
CH_3	−532.3465	−227.1	−229.1	−2.0
$C(CH_3)_3$	−650.2388	−232.5	−231.5	1.0
CF_3	−830.0834	−211.5	−215.8	−4.2
NH_2[1]	−548.3936	−232.3	−232.5	−0.2
Ph	−724.0272	−231.3	−231.3	0.0
$PhCH_2$	−763.3211	−229.6	−231.1	−1.5

[a] The amino protonated form is 34.5 kcal/mol less stable than the 3H and 4H forms.

TABLE 2: Energy Values of Bases (E_B) and Conjugate Acids (E_{3H},E_{4H}) in H_2O ($\epsilon = 80$)

R	base (au)	$E_B - E_{(3H)}$ (kcal/mol)	$E_B - E_{(4H)}$ (kcal/mol)	$E_{(4H)} - E_{(3H)}$ (kcal/mol)
H	−493.0527	−268.9	−269.4	−0.5
CF_3	−830.0949	−259.2	−264.1	−4.9
NH_2[1]	−548.4157	−277.3	−273.2	4.1

[a] The amino protonated form is 17 and 13 kcal/mol less stable than the 3H and 4H forms, respectively.

solvent response. For all calculations we have used the TURBOMOLE 5.7[12] suite of programs.

4. Results and Discussion

4.1. Structure and Energetics of the Basic and Conjugate Acid Forms. The optimized ground state geometry of the basic forms and two conjugate acid (protonated) forms considered are almost C_s symmetry except for the benzyl derivative. In the case of the benzyl derivative, the phenyl ring of the benzyl substituent is in the plane almost perpendicular to the plane of the monophenyl oxadiazole ring. In the case of the amino substituent, we have also considered an additional site of protonation at the amino group.

Optimized ground state energy values for the basic and the two conjugate acid forms are given in Table 1. We observe that all the conjugate acid (protonated) forms have gas-phase proton affinity of around 230 kcal/mol. Analyzing the relative energies of the conjugate acid forms we found that in general 4H forms have energies 1−4 kcal/mol lower than those for the corresponding 3H forms (the only exception is the *tert*-butyl derivative where the 4H form is 1 kcal/mol less stable than the 3H form). These energy differences lie within error of the method, not allowing us to give a definite answer on what site of protonation is energetically preferable. On the other hand, the product of protonation of the amino derivative on the amino group has an energy higher by as much as 34 kcal/mol, suggesting that the NH_2 group is not the preferred site of protonation.

The effect of solvent on the energetics of the basic and conjugate acid forms for H, CF_3 and NH_2 derivatives was investigated and the energy values are given in Table 2. We find that in the presence of a solvent the conclusion is the same: the 4H forms have lower energies than the corresponding 3H forms, but the differences lie within the error of the method.

4.2. Spectral Properties. Experimental absorption and fluorescence spectra of the basic forms of the oxadiazole derivatives are obtained in heptane, sulfuric acid, H_2O, and ethanol solvents. Details of the medium, absorption, emission peaks along with the quantum yield and molar extinction coefficient are tabulated in Table 3. Experimentally, a single band is observed in the absorption spectra. The predicted

TABLE 3: Spectral Data for Base Forms (cm^{-1})

		experimental				gas-phase calculated	
R	medium	ν_{abs}^{max}	ϵ	ν_{fl}^{max}	ϕ	ν_{abs}	ν_{fl}
H	heptane	41200	10800	32700	0.08	39001 (S_2) 38553 (S_1)	33742
	H_2SO_4[a]	40800	9920				
	H_2O			32200	0.13		
CH_3	ethanol	39700	18750	33000	0.13	38176 (S_1)	32981
	heptane	39500	19670	33200	0.09		
	H_2SO_4[b]	40000	17900				
	H_2O			32700	0.22		
$C(CH_3)_3$	heptane	39800	19600	33200	0.08	37819 (S_1)	32558
	H_2SO_4[b]	40000	18500				
	H_2O			33003	0.212		
CF_3	heptane	40323	21300	33223	0.102	38208 (S_2) 37536 (S_1)	33369
	H_2SO_4[c]	39800	13000				
	H_2O			31500	0.16		
NH_2	heptane	36100	13850	30500	0.36	34752 (S_1)	31209
	H_2O	36400	10120	28600	0.09		
Ph[7]	H_2SO_4[d]	35500 42600	21500 6050	29300	0.77	32434 (S_1)	27967
$PhCH_2$	heptane	39700	7500	33200	0.09	37401 (S_1)	31842
	H_2SO_4[d]	39700	17400				
	H_2O			32600	0.15		

[a] 25.7%. $H_0 = -1.50$. [b] 8.7%. $H_0 = -0.30$. [c] 41.0%. $H_0 = -2.59$. [d] 15.8%. $H_0 = -0.82$.

absorbance and the emission peaks of the basic forms are given in Table 3, for absorbance peaks the corresponding excited state is reported in parentheses. The predicted absorbance of the basic forms is in reasonable agreement (average difference is around 2000) with the experimental spectra for all the molecules. From the experimental data we can see that for the basic (neutral) forms the solvent does not affect the positions of the peaks essentially.

4.2.1. Effect of Protonation on the Fluorescence Spectra. The absorption spectra of conjugate acid (protonated) forms are obtained in aqueous solutions of sulfuric acid and are tabulated in Table 4. Protonation leads to red shifts in the absorbance spectra in all the studied derivatives except for the NH_2 where a blue shift is observed. Although the energy differences between the isomeric protonated forms are less than 4 kcal/mol on average, the calculated spectral properties of the 3H and 4H protonated forms differ substantially. Calculated peaks in the absorption spectra of the protonated forms are given in Table 4. For H, CH_3 and NH_2 derivatives, we have calculated spectra with solvent taken into account (as described in section 3). We see (Table 5) that there is relatively small solvatochromic effect, which justifies our use of gas-phase calculated spectral data.

Comparing the absorption maxima of experimental spectra in the acidic media with the calculated absorption peaks of the 3H and 4H forms of conjugate acids (Table 4), we see that, for H, CH_3, $C(CH_3)_3$, NH_2, and $PhCH_2$ substituents, calculated peaks of 3H forms lie closer to the observed maxima than the corresponding 4H forms; for the CF_3 substituents, the reverse is true.

However, our calculations predict a single strong peak for the 4H forms and double peak of lower intensity (oscillator strength) for the 3H forms (except the amino derivative). Thus we conclude that at least for H, CH_3, $C(CH_3)_3$, CF_3 and $PhCH_2$ derivatives 4H forms of conjugate acids are observed experimentally. In most cases the differences between observed and calculated peaks are less than 3300 (0.4 eV), and it is a known fact[14,35−37] that for some systems (especially those with con-

TABLE 4: Spectral Data: Conjugate Acid Forms (cm^{-1})

	experimental				gas-phase calculated			
R	ν_{abs}^{max}	ϵ	ν_{fl}^{max}	ϕ	ν_{abs}^{BH+} (3H)	ν_{abs}^{BH+} (4H)	ν_{fl}^{BH+} (3H)	ν_{fl}^{BH+} (4H)
H[a]	38200	10900	27850	0.07	37830 (S_4) 29482 (S_2)	35508 (S_2)	17565	26804
CH_3[b]	38600	16600	28400	0.15	38201 (S_4) 31145 (S_2)	35353 (S_2)	20837	27849
$C(CH_3)_3$[b]	38300	17600	28500	0.16	38970 (S_4) 33061 (S_2)	35004 (S_2)	22900	28441
CF_3[c]	36200	14900			37328 (S_4)	34924 (S_2)	13852	25701
CF_3[d]			26400	0.04	27016 (S_2)			
NH_2[e]	38500	10240			36037 (S_2)	32307 (S_1)	30161	28424 25360[f]
Ph[b,7]	33900 41000	25000 10700	26200	0.72	35531 (S_4) 27246 (S_1)		20064	
$PhCH_2$[b]	38000	17300	28000	0.018	38606 (S_8) 32490 (S_4)	34728 (S_4)	19121	14105

[a] H_2SO_4 67.3%, $H_0 = -5.52$. [b] H_2SO_4 56.9%, $H_0 = -4.14$. [c] H_2SO_4 77.1%, $H_0 = -7.20$. [d] H_2SO_4 81.2%, $H_0 = -7.65$. [e] H_2SO_4 0.1 M, pH = 1. [f] The NH_3 group is protonated.

TABLE 5: Absorption Peaks of Bases and Conjugate Acids in H_2O ($\epsilon = 80$)

R	ν_{abs}	ν_{abs}^{BH+} (3H)	ν_{abs}^{BH+} (4H)
H	38941 (S_2)	36062 (S_2) 40827 (S_4)	36585 (S_2)
CF_3	37312 (S_2)	39084 (S_4) 31379 (S_2)	35734 (S_2)
NH_2	34311 (S_1)	37436 (S_2) 36920 (S_1)	32357 (S_1) 41196 (S_3) 37209 (S_2)[a]

[a] Protonated at the amino nitrogen.

siderable contribution of ionic valence-bond structure into the excited state wave function) the TDDFT method underestimates the energies of the low-lying HOMO−LUMO excited states by about 0.5 eV.

We have studied the effect of solvent on the absorption spectra of base and conjugate acid forms of H, CF_3 and NH_2 derivatives. For the base forms we find that only one intense peak is observed and the difference with the gas-phase calculation is less than 300. For the conjugate acid forms we find that calculated peaks of 4H forms are closer to the experimentally observed values for R = H and R = CF_3, whereas for the NH_2 derivative the absorption peak of amino protonated form is closer to the experimental value.

4.2.2. Effect of Protonation on the Fluorescence Spectra. Fluorescence spectra of the above oxadiazole derivatives show a single band that is substantially red shifted corresponding to the basic forms. No fluorescence is observed for the NH_2 derivative. For the calculation of the emission peaks of the basic and conjugate acid forms, the lowest bound singlet excited states S_1 of the basic, 3H and 4H forms were optimized using TDDFT methods for excited state properties.[14] When we optimize without symmetry constraints for the lowest singlet excited state for the protonated forms, in a few cases we observe a geometry distortion leading to convergence problems. Thus we optimized the lowest singlet excited states for the conjugate acid (protonated) forms with the C_s symmetry constraint (except the benzyl derivative, where we constrained the planarity of oxadiazole ring). We observed that the excited state geometries of the basic and protonated forms are close to the C_s symmetry of the corresponding ground state geometries. The predicted emission peaks for the 3H and 4H forms are tabulated in Table 4.

Experimentally, fluorescence of the basic form is red shifted by higher than 50 nm on protonation. Calculated emission spectra of 3H forms differ substantially from the experimental values. We do find the fluorescence of the NH_2 derivative with the emission peaks at 30 161, 28 424, and 25 360 for the 3H, 4H, and amino-protonated forms, respectively. Emission peaks of 4H forms of H, CH_3, $C(CH_3)_3$, and CF_3 derivatives are in good agreement with the experimental values (differences are less than 1200). For the phenyl and benzyl derivatives, there are large differences between the calculated and experimental peaks.

4.3. Preferred Conjugate Acid Forms by Density Descriptors. Analyzing the change in local Mulliken charges on the basic centers of oxadiazole as a function of change in number of electrons, we have obtained the condensed local softness values for the N(3) (for 3H form) and N(4) (for 4H form) nitrogen atoms of oxadiazoles to predict the dominant conjugate acid forms.

The condensed to atoms local softness values s_k^- are presented in Table 6. A higher value of s_k^- suggests the most probable site of protonation. Analyzing the s_k^- values for the basic forms in the ground state, we see that the descriptors approach predicts the 4H form to be the preferred form for H, CH_3, $C(CH_3)_3$, CF_3, and $PhCH_2$ derivatives and the amino protonated form and 3H form for the NH_2 derivative. We have verified that charges calculated using a smaller basis set (6-31G*) give very close values of Fukui function indices and lead to the same prediction. Thus, on the basis of local descriptors approach for the ground state of the basic forms, we conclude that the 4H form is the predominant conjugate acid form in most of the derivatives, excluding the amino derivative.

To analyze the predominant conjugate acid form contributing to the intense peak in the fluorescence spectra, we have also calculated local softness values for the excited state using the finite approximation method at the optimized excited state geometry. The condensed to atoms local softness values are presented in Table 7. On the basis of local softness values, we observe that the 4H form is preferred for H, CH_3, $C(CH_3)_3$, and CF_3 derivatives and the 3H form is preferred for $PhCH_2$ and NH_2 derivatives. Compared to the case with the ground state local softness values, a different site of protonation is predicted for the benzyl derivative. Thus the local density descriptors results are concurrent with the fluorescence spectral predictions in most cases.

4.4. Leading Transitions in the Absorption Spectra of Basic and Conjugate Acid Forms. General structures of low-lying orbitals participating in leading transitions for basic and conjugate acid forms are illustrated in Figures 2 and 3.

TABLE 6: Mulliken Charges and Local Softness Values for the Ground State

	charges				
atom	neutral	anion	cation	f_k^-	s_k^-
		R = H			
N(3)	−0.111	−0.153	−0.043	0.067	0.209
N(4)	−0.053	−0.120	0.032	0.085	0.266
O(1)	−0.133	−0.171	−0.094	0.039	0.122
		R = CH_3			
N(3)	−0.087	−0.123	−0.018	0.070	0.223
N(4)	−0.066	−0.136	0.018	0.083	0.265
O(1)	−0.137	−0.174	−0.098	0.040	0.128
		R = $(CH_3)_3C$			
N(3)	−0.062	−0.095	0.010	0.071	0.231
N(4)	−0.075	−0.144	0.002	0.077	0.250
O(1)	−0.113	−0.148	−0.074	0.039	0.127
		R = CF_3			
N(3)	−0.034	−0.087	0.023	0.057	0.182
N(4)	−0.053	−0.113	0.030	0.083	0.265
O(1)	−0.103	−0.151	−0.067	0.036	0.115
		R = NH_2			
N(3)	−0.148	−0.179	−0.041	0.106	0.354
N(4)	−0.066	−0.146	0.000	0.066	0.220
O(1)	−0.169	−0.200	−0.125	0.044	0.147
N(a)	−0.362	−0.392	−0.250	0.112	0.374
		R = Ph			
N(3)	−0.075	−0.111	−0.016	0.059	0.218
N(4)	−0.074	−0.110	−0.016	0.059	0.218
O(1)	−0.130	−0.164	−0.103	0.027	0.100
		R = $PhCH_2$			
N(3)	−0.075	−0.104	−0.025	0.050	0.168
N(4)	−0.072	−0.130	−0.009	0.063	0.212
O(1)	−0.121	−0.154	−0.096	0.025	0.084

TABLE 7: Mulliken Charges and Local Softness Values for the Excited State

	charges				
atom	neutral	anion	cation	f_k^-	s_k^-
		R = H			
N(3)	−0.129	−0.148	−0.021	0.108	0.372
N(4)	−0.058	−0.169	0.096	0.155	0.535
O(1)	−0.133	−0.209	−0.059	0.074	0.255
		R = CH_3			
N(3)	−0.110	−0.113	−0.103	0.007	0.025
N(4)	−0.069	−0.192	−0.012	0.057	0.201
O(1)	−0.136	−0.210	−0.116	0.020	0.071
		R = $(CH_3)_3C$			
N(3)	−0.086	−0.084	−0.063	0.023	0.083
N(4)	−0.074	−0.196	−0.025	0.049	0.177
O(1)	−0.111	−0.187	−0.090	0.022	0.080
		R = CF_3			
N(3)	−0.026	−0.053	0.049	0.075	0.262
N(4)	−0.070	−0.144	0.091	0.161	0.563
O(1)	−0.098	−0.190	−0.034	0.064	0.224
		R = NH_2			
N(3)	−0.196	−0.217	−0.006	0.190	0.687
N(4)	−0.048	−0.245	0.045	0.093	0.336
O(1)	−0.172	−0.292	−0.088	0.084	0.304
N(a)	−0.417	−1.030	−0.209	0.208	0.752
		R = Ph			
N(3)	−0.081	−0.083	0.028	0.109	0.446
N(4)	−0.081	−0.083	0.027	0.109	0.446
O(1)	−0.125	−0.185	−0.075	0.050	0.205
		R = $PhCH_2$			
N(3)	−0.079	−0.095	0.039	0.118	0.439
N(4)	−0.072	−0.158	0.014	0.086	0.320
O(1)	−0.115	−0.199	−0.063	0.053	0.197

We observe that the leading transition contributing to the intense peak in the absorption spectra of the basic form is a HOMO to LUMO transition. HOMO and LUMO orbitals of the basic forms are predominantly oxadiazole π-orbital mixed with the phenyl π-orbitals. On protonation, the mixed oxadiazole−phenyl π-orbital is stabilized and becomes the HOMO−1 orbital. The leading transition contributing to the intense peak in the absorption spectra is due to the transitions from this mixed oxadiazole orbital and thus in all the protonated spectra S_2 and S_4 transitions are the intense transitions. All the transitions are stabilized on protonation leading to the observed red shifts even from the $S_0 \rightarrow S_2$ and $S_0 \rightarrow S_4$ transitions.

4.5. Substituent Effects on Spectra: Differential Density Map Analysis. *4.5.1. Fluorescence Spectra of Acid Forms: Substituent Effects.* Differential density maps are presented in Figure 4 (drawn by the gOpenMol[38,39] software). Red and green colors indicate a decreased and an increased density in the excited state, respectively. The differential density maps have been calculated at the optimized ground state (S_0) geometries of the base forms. The differential density maps between the ground and excited state corresponding to the most intense peak in the absorption spectra of base forms have been calculated.

We find that H, CH_3, and $(CH_3)_3C$ substituents are practically not involved in the excited state density redistribution. We observe that the substituents CF_3, NH_2, Ph and $PhCH_2$ do participate in the density redistribution. The phenyl and benzyl substituents participate as π-donors, and the amino group participates more as a π-donor than as a σ-acceptor. In the case of the CF_3 derivative, the participation is through the polarizable p-type orbitals of F atom. The 5-phenyl ring acts mostly as a π-donor and the electron density concentrates mainly on the C(5)−phenyl bond.

From the above observations we see that a distinct effect on the substituted oxadiazole spectra is expected from the substituents having lone pairs or flexible π-systems (i.e., substituents characterized by M-effect).

4.5.2. Fluorescence Spectra of Acid Forms: Substituent Effects. To understand the reasons for the differing red shifts observed in the fluorescence spectra of the 3H and 4H forms, we have studied the excited state differential density maps of the H, CF_3 and phenyl derivatives. Differential density maps are presented in Figure 5 (drawn by the gOpenMol[38,39] software).

Red and green colors indicate a decreased and an increased density in the excited state, respectively. The maps have been calculated at the optimized excited state (S_1) geometries of the 3H, 4H forms and correspond to the emission peak in the fluorescence spectra of the 3H, 4H conjugate acid forms, respectively.

From the differential density maps we see that the substituents do participate in the excited state density redistribution. In comparison with the basic forms, there is an increase in the electron density on the oxadiazole ring and on the N−H bond in particular, stabilizing the 3H and 4H forms. We observe that there is a marked increase in the inflow of electron density to the N−H bond in 3H form, stabilizing it more in comparison with the 4H form in the excited state. Thus there is a higher red shift in emission peak of the 3H form.

5. Summary and Conclusions

The basic and conjugate acid forms of 2-R-5-phenyl-1,3,4-oxadiazoles have been investigated by extensive calculations. The ground states of the optimized structures of the basic and conjugate acid forms of all the derivatives except the benzyl derivative are close to C_s symmetry. Analysis of energy

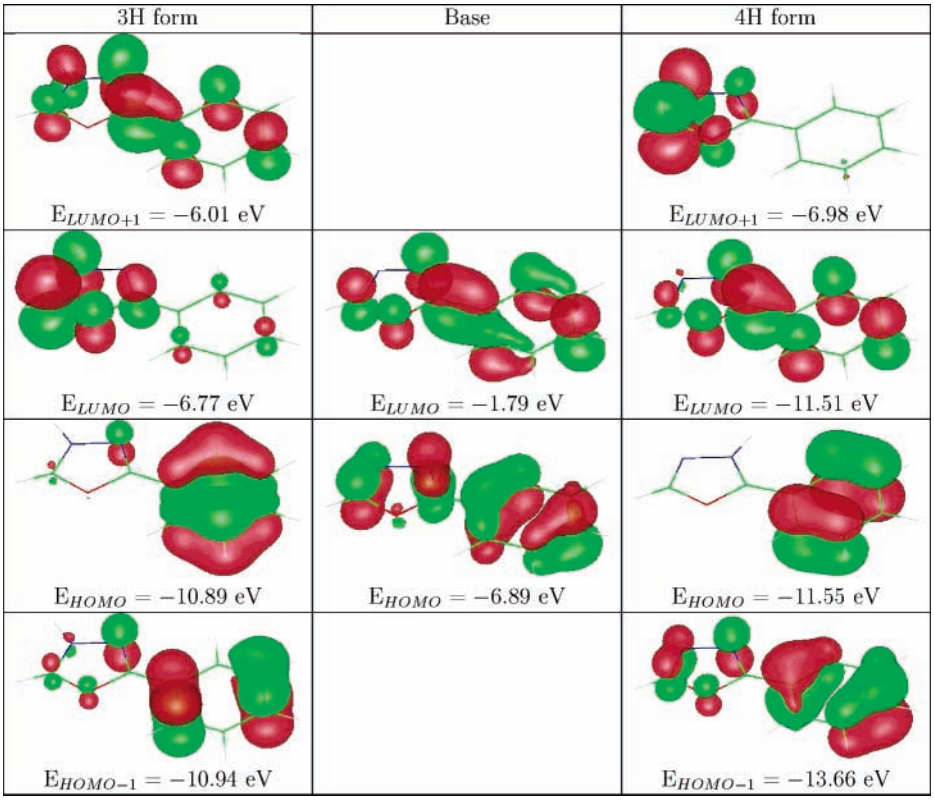

Figure 2. Orbitals: basic and conjugate acid forms of R = H.

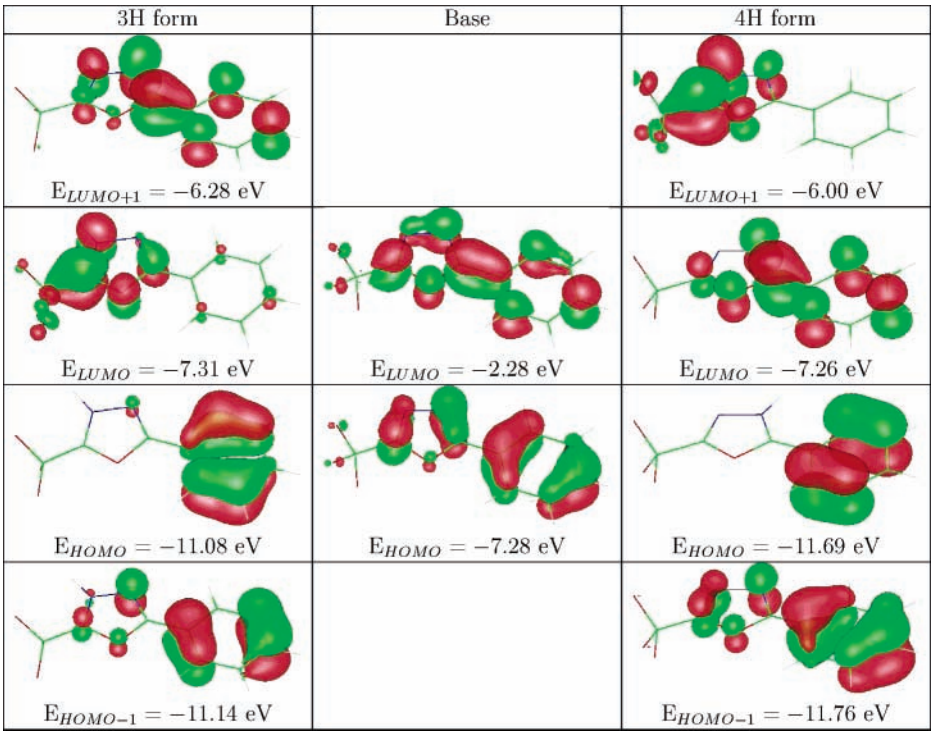

Figure 3. Orbitals: basic and conjugate acid forms of R = CF_3.

differences between the basic form and two possible conjugate acid forms, both in the gas phase and in the presence of solvent, does not allow one to draw a definite conclusion.

Experimental absorption spectra were taken in different solvents and a red shift was observed in acidic media due to the formation of the conjugate acid forms.

Calculated absorption maxima are in agreement with the experimental values and from the calculated absorption spectra we see that the 3H form is characterized by multiple peaks of comparable intensity, whereas the 4H form spectra are characterized by a single intense peak. The relative basicity of the oxadiazole nitrogen atoms are studied using the density descriptors approach and the local softness values indicate that the 4H form is the more preferred form in all cases except the NH_2 derivative. Analyzing the orbitals involved in the leading transitions in the basic and conjugate acid forms, it is seen that the leading transition is from the mixed oxadiazole−phenyl orbital, which is stabilized on protonation, making $S_0 \rightarrow S_2$, S_4

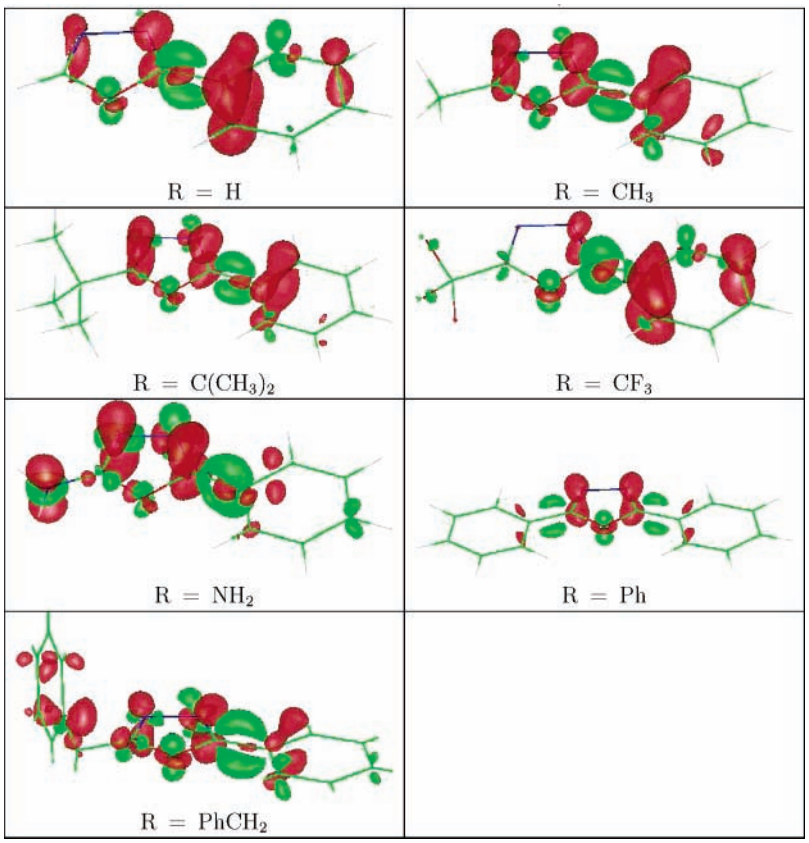

Figure 4. Differential density maps: oxadiazoles (base forms).

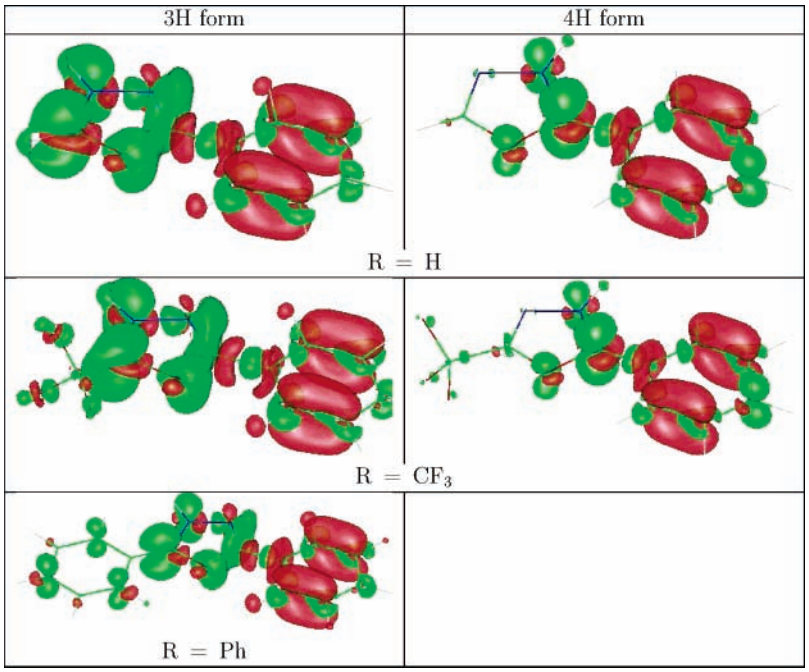

Figure 5. Differential density maps: oxadiazoles (acid forms).

transitions intense in the absorption spectra of acid forms. Comparing the excited state density redistribution at the ground state geometry of the oxadiazole derivatives, one sees that only substituents having a lone pair or flexible π-systems have a distinct effect on the oxadiazole absorption spectra.

Experimental fluorescence spectra were taken in aqueous sulfuric acid solutions and there is a high red shift on protonation. The lowest singlet excited state S_1 of the 3H and 4H forms of the oxadiazole derivatives were optimized and the structures are found to be similar to the geometry of the corresponding ground states. In contrast to the absorption spectra, the emission peaks of the 3H and 4H forms differ largely with the 3H form highly red shifted in comparison to the 4H form. For the amino group, experimentally, fluorescence is not observed, and theoretical calculations predict the emission peak of the conjugate acid form to be around 30 000. Calculated emission peaks for the 4H forms are in good agreement with the experimental observations except for the phenyl and benzyl

derivatives. Local descriptors were calculated at the excited state geometry and the local softness values suggest the 4H form to be the preferred form for all derivatives except for the benzyl and amino derivatives. Compared to the ground state predictions, there is a reverse trend seen for the benzyl derivative. Comparing the excited state density redistribution at the S_1 geometry, one sees that the substituents have an effect on the oxadiazole fluorescence spectra. Possible reasons for the differing red shifts of the 3H and 4H protonated forms were investigated by studying the excited state differential density at the optimized S_1 geometry and it is seen that there is an increased stabilization of the N−H bond in the excited state in case of the 3H form in comparison with the 4H form and it is probably responsible for the higher red shift observed in case of the 3H form of the conjugate acid.

Supporting Information Available: Low-lying excitation energies with oscillator strengths, and leading transitions for the basic and acid forms of the oxadiazole derivatives are tabulated. Mulliken charges, Fukui functions and local softness values calculated in smaller basis (6-31G*) are reported. Experimental absorption and fluorescence spectra graphs as well as calculated spectra in the form of overlapping Gaussians, simulating solvent broadening, are also supplied.

Acknowledgment. A.V.G and A.D thank Lunarc computational facility at the Lund University, Sweden, for computational support.

References and Notes

(1) Boschelli, D. H.; Connor, D. T.; Bornemeir, D. A.; Dyer, R. D.; Kennedy, J. A.; Kuipers, P. J.; Okonkwo, G. C.; Schrier, D. J.; Wright, C. D. *J. Med. Chem.* **1993**, *36*, 1802−1810.

(2) Santagati, M.; Modica, M.; Santagati, A.; Russo, F.; Caruso, A.; Cutili, V.; Pietor, E. D.; Amico-Roxas, M. *Pharmazie* **1994**, *12*, 880−884.

(3) Tamoto, N.; Adachi, C.; Nagai, K. *Chem. Mater.* **1997**, *9*, 1077−1085.

(4) Hu, Y.; Zhang, Y.; Wang, F. L. L.; Ma, D.; Jing, X. *Synth. Met.* **2003**, *137*, 1123−1124.

(5) Wang, J. F.; Jabbour, G. E.; Mash, E. A.; Anderson, J.; Zhang, Y.; Lee, P. A.; Armstrong, N. R.; Peyghambarian, N.; Kippelen, B. *Adv. Mater.* **1999**, *11*, 1266−1269.

(6) Antoniadis, H.; Inbasekaran, M.; Woo, E. P. *Appl. Phys. Lett.* **1998**, *73*, 3055−3057.

(7) Trifonov, R. E.; Rtishchev, N. I.; Ostrovskii, V. A. *Spectrochim. Acta, Part A* **1996**, *52*, 1875−1882.

(8) Meot-Ner, M.; Liebman, J. F.; Del-Bene, J. E. *J. Org. Chem.* **1986**, *51*, 1105.

(9) Trifonov, R. E.; Ostrovskii, V. A. *Russ. J. Org. Chem.* **2001**, *37*, 416−420.

(10) Doroshenko, A. O.; Posokhov, E. A.; Verezubova, A. A.; Ptyagina, L. M.; Skripkina, V. T.; Shershukov, V. M. *Photochem. Photobiol. Sci.* **2002**, *1*, 92.

(11) Kenny, P. W. *J. Chem. Soc., Perkin Trans. 2* **1994**, *2*, 199−202.

(12) Bauernschmitt, R.; Haeser, M.; Treutler, O.; Ahlrichs, R. *Chem. Phys. Lett.* **1997**, *264*, 573−578.

(13) Treutler, O.; Ahlrichs, R. *J. Chem. Phys.* **1995**, *102*, 346−354.

(14) Furche, F.; Ahlrichs, R. *J. Chem. Phys.* **2002**, *117*, 7433−7447.

(15) Bauernschmitt, R.; Ahlrichs, R. *J. Chem. Phys.* **1996**, *104*, 9047−9052.

(16) Bauernschmitt, R.; Ahlrichs, R. *Chem. Phys. Lett.* **1996**, *256*, 454−464.

(17) Parr, R. G.; v. Szentpaly, L.; Liu, S. *J. Am. Chem. Soc.* **1999**, *121*, 1922.

(18) Domingo, L. R.; Aurell, J. M.; Pérez, P. *J. Phys. Chem. A* **2002**, *106*, 6871.

(19) Roy, R. K.; Krishnamurti, S.; Geerlings, P.; Pal, S. *J. Phys. Chem. A* **1998**, *102*, 3746−3755.

(20) W. Yang, R. G. P. *Proc. Natl. Acad. Sci. U.S.A* **1985**, *82*, 4049.

(21) Deka, R. C.; Ajitha, D.; Hirao, K. *J. Phys. Chem. A* **2003**, *107*, 8574−8577.

(22) Roy, R. K. *J. Phys. Chem. A* **2004**, *108*, 4934−4939.

(23) Roy, R. K.; Usha, V.; Paulovic, J.; Hirao, K. *J. Phys. Chem. A* **2005**, *109*, 4601−4606.

(24) Becke, A. D. *Phys. Rev. A* **1988**, *38*, 3098−3100.

(25) Perdew, J. P. *Phys. Rev. B* **1988**, *33*, 8822−8824.

(26) Dirac, P. A. M. *Proc. Royal Soc. (London) A* **1929**, *123*, 714.

(27) Slater, J. C. *Phys. Rev.* **1951**, *81*, 385−390.

(28) Vosko, S.; Wilk, L.; Nussair, M. *Can. J. Phys.* **1980**, *58*, 1200.

(29) Schfer, A.; Huber, C.; Ahlrichs, R. *J. Chem. Phys.* **1994**, *100*, 5829−5835.

(30) Schfer, A.; Horn, H.; Ahlrichs, R. *J. Chem. Phys.* **1992**, *97*, 2571−2577.

(31) Lee, C.; Yang, W.; Parr, R. G. *Phys. Rev. B* **1988**, *37*, 785−789.

(32) Becke, A. D. *J. Chem. Phys.* **1993**, *98*, 5648−5652.

(33) Schafer, A.; Klamt, A.; Sattel, D.; Lohrenz, J. C. W.; Eckert, F. *Phys. Chem. Chem. Phys.* **2000**, *2*, 2187−2193.

(34) Kundrat, M. D.; Autchbach, J. *J. Phys. Chem. A* **2006**, *110*, 4115−4123.

(35) Grimme, S.; Parac, M. *Chem. Phys. Chem.* **2003**, *4*, 292−295.

(36) Parac, M.; Grimme, S. *Chem. Phys.* **2003**, *292*, 11−21.

(37) Fabiano, E.; Sala, F. D.; Weimer, R. C. M.; Gorling, A. *J. Phys. Chem. A* **2005**, *109*, 3078−3085.

(38) Laaksonen, L. *J. Mol. Graph.* **1992**, *10*, 33−34.

(39) Bergman, D. L.; Laaksonen, L.; Laaksonen, A. *J. Mol. Graph. Model.* **1997**, *15*, 301−306.